Atmospheric Research 200 (2018) 88–96

Contents lists available at ScienceDirect

Atmospheric Research

journal homepage: www.elsevier.com/locate/atmosres

Most probable mixing state of aerosols in Delhi NCR, northern India

Parul Srivastava[a], Sagnik Dey[a,*], Atul Kumar Srivastava[b], Sachchidanand Singh[c], Suresh Tiwari[b]

[a] Centre for Atmospheric Sciences, Indian Institute of Technology Delhi, Hauz Khas, New Delhi 110016, India
[b] Indian Institute of Tropical Meteorology (Delhi Branch), Prof. Ramnath Vij Marg, New Delhi 110060, India
[c] Radio & Atmospheric Sciences Division, National Physical Laboratory, Dr. K. S. Krishnan Marg, New Delhi 110012, India

ABSTRACT

Unknown mixing state is one of the major sources of uncertainty in estimating aerosol direct radiative forcing (DRF). Aerosol DRF in India is usually reported for external mixing and any deviation from this would lead to high bias and error. Limited information on aerosol composition hinders in resolving this issue in India. Here we use two years of aerosol chemical composition data measured at megacity Delhi to examine the most probable aerosol mixing state by comparing the simulated clear-sky downward surface flux with the measured flux. We consider external, internal, and four combinations of core-shell (black carbon, BC over dust; water-soluble, WS over dust; WS over water-insoluble, WINS and BC over WINS) mixing. Our analysis reveals that choice of external mixing (usually considered in satellite retrievals and climate models) seems reasonable in Delhi only in the pre-monsoon (Mar-Jun) season. During the winter (Dec-Feb) and monsoon (Jul-Sep) seasons, 'WS coating over dust' externally mixed with BC and WINS appears to be the most probable mixing state; while 'WS coating over WINS' externally mixed with BC and dust seems to be the most probable mixing state in the post-monsoon (Oct–Nov) season. Mean seasonal TOA (surface) aerosol DRF for the most probable mixing states are 4.4 ± 3.9 (-25.9 ± 3.9), -16.3 ± 5.7 (-42.4 ± 10.5), 13.6 ± 11.4 (-76.6 ± 16.6) and -5.4 ± 7.7 (-80.0 ± 7.2) W m^{-2} respectively in the pre-monsoon, monsoon, post-monsoon and winter seasons. Our results highlight the importance of realistic mixing state treatment in estimating aerosol DRF to aid in policy making to combat climate change.

1. Introduction

Aerosol direct radiative forcing (DRF) has large uncertainty due to various factors like error in composition, scale height, mixing state, particle morphology etc. (Boucher et al., 2013). Aerosols which are emitted from a variety of sources are mixed in different ways during its transport, thus changing their optical properties (Chandra et al., 2004; Dey et al., 2008; Srivastava and Ramachandran, 2013). In external mixing, different aerosol species (each particle is of homogeneous composition) do not interact with each other physically or chemically (case 1 in Fig. 1). One extreme is internal mixing (Case 2 of Fig. 1), where particles of homogeneous composition are mixed internally so that the composition of each composite particle is weighted average of individual homogeneous particles. In between, we have core-shell mixing (remaining cases in Fig. 1), where one particular species (e.g. dust) is coated by another species (e.g. black carbon, BC). Observations suggest that fully internal mixing may not be realistic, rather the reality is somewhere between external and core-shell mixing or a combination of the two (Jacobson et al., 2000). Therefore, it is important to understand the role of mixing state in modulating aerosol DRF (Jacobson, 2001; Wang et al., 2010) and its feedback on atmosphere, especially at regional scale where aerosol characteristics are highly variable.

Indian subcontinent has been identified as a regional aerosol hotspot and one such place, where aerosol optical depth (AOD) shows large seasonal and spatial variability depending on the synoptic meteorology, emission characteristics and topography (Dey and Di Girolamo, 2010 and the references therein). Contrary to a decreasing global trend (Mishchenko et al., 2007), AOD shows an increasing trend in India in the recent times (Dey et al., 2011; Krishna Moorthy et al., 2013), therefore making aerosols a critical component in understanding the regional climate variability (Sanap and Pandithurai, 2015).

Direct measurement of aerosol composition covering all seasons continuously at one location is limited in the Indian subcontinent. In absence of detailed aerosol composition, researchers mostly use an indirect approach to estimate top-of-the-atmosphere (TOA) and surface DRF. Aerosol composition is inferred through an iterative process, where the respective number concentrations of individual species are

* Corresponding author.
E-mail address: sagnik@cas.iitd.ac.in (S. Dey).

http://dx.doi.org/10.1016/j.atmosres.2017.09.018
Received 13 February 2017; Received in revised form 14 September 2017; Accepted 27 September 2017
Available online 07 October 2017
0169-8095/

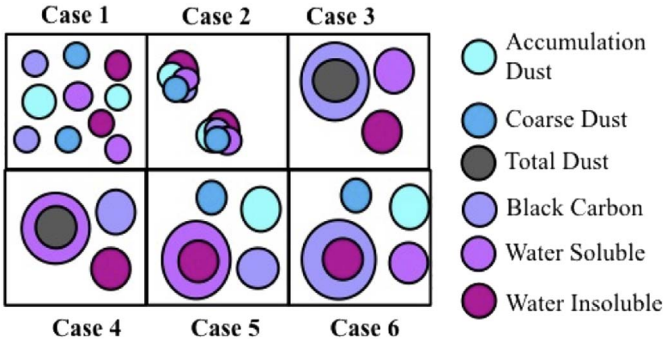

Fig. 1. Illustration of various mixing states. Case 1 and Case 2 represent external mixing and internal mixing respectively. Case 3, Case 4, Case 5, and Case 6 represent core-shell mixing of 'BC over dust externally mixed with WS and WINS', 'WS over dust externally mixed with BC and WINS', 'WS over WINS externally mixed with dust and BC' and 'BC over WINS externally mixed with dust and WS' respectively.

tuned by matching the spectral AOD calculated by Mie theory with direct measurements, either by ground-based radiometers (e.g. Singh et al., 2005; Dumka et al., 2014; More et al., 2013) or satellite-derived aerosol products (Dumka et al., 2014; More et al., 2013). The spectral optical properties are then utilized for estimating aerosol DRF using radiative transfer model (e.g. Singh et al., 2005; Dey and Tripathi, 2008; Singh et al., 2010; Srivastava et al., 2012; Srivastava et al., 2014b). External mixing state is usually considered for calculating aerosol spectral optical properties in such cases and therefore any error due to wrong choice of mixing state (i.e. if mixing state deviates from external mixing in reality) infiltrates into the aerosol DRF estimate. In addition, the accuracy of inferred composition from such process depends on robustness of matching criteria and choice of individual species in bulk aerosol composition. Therefore, it is difficult to ascertain the probable mixing state, when inferred composition itself has large uncertainty.

Aerosol optical properties are well studied in the western IGB (Tiwari et al., 2015). For example, Lodhi et al. (2013) examined AOD climatology, seasonal variability and trend for the period 2001–2012 at Delhi NCR using long-term ground-based measurements, while Srivastava et al. (2014a) established satellite-based aerosol climatology for the last decade. In another study, Srivastava et al. (2014b) characterized major aerosol types in Delhi NCR using a combination of fine-mode fraction and single scattering albedo (SSA). Diurnal and seasonal variations of carbonaceous aerosols and their emission sources were also examined at Delhi (Srivastava et al., 2014b; Tyagi et al., 2017). Singh et al. (2010) estimated 'clear-sky' aerosol DRF over Delhi for one year period using AOD spectrum measured by a passive radiometer and other optical properties (e.g. SSA and asymmetry parameter) estimated by Optical Properties of Aerosols and Clouds (OPAC) model. Key findings of these studies can be summarized as follows: (1) AOD peaks during the pre-monsoon season (Mar–Jun) along with a reduction in Angstrom parameter indicating an increase in coarse dust particles in columnar burden; (2) AOD continues to remain high during the dry phase of monsoon (Jul–Sep) season because of persistent dust transport and high anthropogenic emission; however measurement of AOD by passive sensor is biased towards 'clear-sky' condition and fails to quantify the washout by rain; (3) dust is ubiquitously present in Delhi NCR with varying source seasonally; (4) absorbing BC shows strong seasonal and diurnal variation with highest value observed during the winter (Dec-Feb) season because of stable boundary layer; (5) concentration of aerosols smaller than 10 μm (PM_{10}) and 2.5 μm ($PM_{2.5}$) is 5 times larger than the Indian air quality standard and 20 times than World Health Organization standard; and (6) very large aerosol DRF at TOA (varies from -1.4 ± 0.4 to $21 \pm 2\ W\ m^{-2}$) and surface (varies from -46 ± 8 to $-110 \pm 20\ W\ m^{-2}$) are observed. All these studies assumed 'external mixing' in computing optical properties and DRF. If aerosol mixing state is not external throughout the year, previous estimates would have large uncertainty. Previous attempts to infer aerosol mixing state in the Indo-Gangetic Basin have focused on the central and eastern parts of the Indo-Gangetic Basin (IGB) (Dey et al., 2008; Srivastava and Ramachandran, 2013). These studies considered spectral aerosol optical properties retrieved by AERONET sunphotometer to constrain inferred aerosol composition. Here, we focus on Delhi national capital region (NCR), in the western part of the IGB.

In the present study, we take advantage of detailed chemical measurement of aerosol samples collected at Delhi NCR for a two-year (2007–2008) period. These data are used to estimate the aerosol DRF in 'clear-sky' condition. Further, we examine the modulation of surface reaching flux by different mixing states and compare with in-situ measurement to infer the most probable aerosol mixing state in each season. Our results provide an insight into the importance of treatment of appropriate mixing state in estimation of aerosol DRF.

2. Approach

Our approach has the following major steps. First, we group the chemical data quantitatively into four major aerosol types. Aerosol spectral optical properties are calculated for various mixing states as described in the following sub-sections. The optical properties are used as inputs to a radiative transfer model to estimate 'clear-sky' aerosol DRF at the TOA and surface. Finally, the surface reaching 'clear-sky' flux in presence of aerosols for various mixing states is compared against measured flux to infer the most probable mixing state of aerosols in this region.

2.1. Aerosol chemical composition

PM_{10} aerosol samples were collected once every week for 24-hour duration in Delhi NCR during the period 2007–2008 to study the chemical composition and its seasonal variation. The chemical data consist of various ions (e.g. Cl^-, NO_3^-, SO_4^-, Na^+, NH_4^+, K^+, Mg^+, Ca^+) and elements (Na, Mg, Al, Si, P, S, Cl, K, Ca, Ti, V, Cr, Mn, Fe, Ni, Cu, Zn, As, Br, Sr, Ba, Pb) along with total PM_{10} mass concentration. Aerosol samples were collected on Whatman Teflon Microfiber filter papers (47 mm diameter, 2.0 μm pore size) using a PM_{10} aerosol sampler (APM 541, Envirotech Pvt. Ltd. India) for 24-hour period. The flow rate of the sampler was $1\ m^3\ h^{-1}$. Particulate matter collected on Teflon filters was extracted in de-ionized water and analyzed by ion chromatography (IC model DX–100, Dionex) for various ions including major cations and anions, as mentioned above. The filters were analyzed by ED–XRF (energy dispersion X–ray fluorescence), a non–destructive method for the determination of major elements. The details about the sampling and the analytical procedures followed for the analysis of aerosol chemical composition are given elsewhere (Perrino et al., 2011).

BC was measured by an Aethalometer (AE-21, Magee Scientific, USA). Aethalometer provides a real-time measurement of the mass concentration of BC aerosols in an air stream using continuous filtration and optical measurement method based on differential absorption method. It was operated at a mass flow rate of $2\ l\ min^{-1}$ and at a time interval of 5 min. Details of Aethalometer working principle and uncertainty in measured BC are discussed in the literature (Hansen et al., 1984; Weingartner et al., 2003; Singh et al., 2010; Collaud Coen et al., 2010; Srivastava et al., 2014b). Aethalometer uses $16.6\ m^2\ g^{-1}$ mass absorption efficiency, which may contribute to uncertainty in estimated BC mass. In addition, multiple scattering of light at the filter fibres and instrumental response with increased particle loading on the filter (shadowing effect) can cause error in BC mass (Virkkula et al., 2015). Using procedure mentioned in Virkkula et al. (2007, 2015) we have estimated compensation parameter k that is used to correct BC mass concentrations measured by the Aethalometer. The average and standard deviation of the last attenuation values estimated by the aethalometer before filter spot changes for wavelength 520 and 880 nm were

53.6 ± 2.7 and 33.2 ± 2.6 respectively. k values estimated are 0.003 ± 0.01 and 0.002 ± 0.1 for wavelength 520 and 880 nm respectively. On an average, BC mass differs maximum by ~5.6% relative to uncorrected BC mass.

Aerosol composition is broadly categorized into four species - BC, dust (in accumulation and coarse mode), water-soluble (WS) and water-insoluble (WINS). Total dust mass has been estimated from measured 'Al' concentration Tare et al. (2006). Dust is further divided into accumulation and coarse mode using size fraction information from MISR sensor on-board TERRA satellite (Dey and Di Girolamo, 2010). According to MISR aerosol algorithm (Kahn et al., 2010), medium and large mode particles (non-spherical shape) are mainly dust. We partition total dust mass in a way that the ratio of optical depths of medium and large particles assuming external mixing (to be consistent with MISR algorithm) match with the corresponding monthly climatological value from MISR over Delhi NCR (Srivastava et al., 2014a). Organic carbon (OC), which includes both WS and WINS components, is estimated by summing up all the elements individually after subtracting the masses from their ion counterparts. Total mass of the elements, ions, BC and dust at accumulation and coarse mode are subtracted from measured PM_{10} mass and the difference is attributed to OC. We note that ~35% of OC is water-soluble organic carbon (WSOC) in the IGB (Ram and Sarin, 2010). Hence, total WS mass is estimated by summing mass of ions and estimated WSOC. Remaining OC mass, which comprises of insoluble fraction, is added to mass of elements to obtain total mass of WINS.

We note that this assumption may lead to uncertainty in estimated dust mass. Recently Samiksha et al. (2017) have shown that Si/Al ratio in road dust varies in India. Any Si/Al ratio different than the upper continental crustal composition (UCC) implies enrichment due to anthropogenic factors. In Delhi, dust is usually transported from the Great Indian Desert and other arid regions in the middle-east Asia during the pre-monsoon (Mar-Jun) and monsoon (Jul-Sep) seasons (Lodhi et al., 2013) and therefore during these seasons, the uncertainty in estimated dust mass is expected to be low. In the post-monsoon (Oct–Nov) to winter season, the source of dust is primarily local (re-suspended) and hence using Si/Al ratio close to UCC reference may lead to uncertainty in dust mass. A ratio higher than reference UCC value implies that the dust mass would be under-estimated. In that case, WINS and WS would be over-estimated. Unless the seasonal variation in Si/Al ratio is quantified, this issue will remain unresolved.

The monthly aerosol chemical composition is summarized in Table 1. BC and dust vary in the range 3.8–28.3 μg/m^3 and 16.8–47.5 μg/m^3 respectively. WS particles show largest range (20–90.5 μg/m^3) while WINS particles vary within 30.5–56.2 μg/m^3. Seasonal variation of mass fractions of the individual aerosol species is illustrated in Fig. 2. BC mass fraction reduces from 18% in winter to 5% in the monsoon season. Similar type of seasonal variation has earlier been reported from other parts of India (e.g., Tripathi et al., 2007; Ramachandran and Kedia, 2010; Safai et al., 2014). Dust mass fraction is higher in the pre-monsoon (24%) and monsoon (25%) seasons relative to the winter (14%) and post-monsoon (14%) (Oct–Nov) seasons. Though the mass fraction of dust is almost similar in the pre-monsoon and monsoon seasons, its absolute mass decreases by 30–50% in the monsoon season (Table 1) due to washout. Ubiquitous presence of dust in aerosol load at Delhi NCR throughout the year is unique in the context of urban aerosol characteristics commonly observed across the world. WINS has the largest contribution (41%–48%) to the total aerosol mass in Delhi NCR with a low seasonal cycle, followed by WS components (25–29%). The observed aerosol composition (summarized in Table 1) is directly utilized to estimate spectral aerosol optical properties assuming various probable mixing states in 'clear-sky' condition.

Table 1
Mean monthly mass concentrations (μg/m^3) of BC, WINS, WS, Dust in accumulation mode ($Dust_{acc}$) and Dust in coarse mode ($Dust_c$) in Delhi.

	BC	WINS	WS	$Dust_{acc}$	$Dust_c$
Jan	21.3	86.7	53.2	8.3	18.8
Feb	24.0	30.5	20.0	5.0	11.8
Mar	8.1	80.5	46.1	8.8	17.1
Apr	6.2	59.1	38.8	13.1	23.0
May	8.2	80.1	42.6	16.7	25.3
Jun	6.9	66.1	32.2	17.4	30.1
Jul	3.8	31.6	24.0	8.0	11.8
Aug	4.1	45.1	23.8	8.5	15.0
Sep	6.4	43.4	27.8	10.1	16.6
Oct	9.8	156.2	90.5	18.2	29.8
Nov	33.9	124.3	79.9	12.7	24.8
Dec	28.3	102.4	67.5	6.0	13.7

2.2. Aerosol mixing state

We consider three types of mixing states - external mixing, core-shell and internal mixing (Fig. 1) for our study. The frameworks of each mixing state are described in the following sections.

2.2.1. External mixing

For the external mixing, number concentrations of the individual aerosol species are calculated from the measured mass and are used as input to OPAC model (Hess et al., 1998) to calculate the spectral AOD, SSA and asymmetry parameter (g). Aerosol scale height and thickness of aerosol layer for each month, two key inputs to the radiative transfer model, are taken from the CALIOP-derived climatology reported in our earlier study (Srivastava et al., 2014a). We analyze CALIOP-retrieved daytime aerosol vertical profiles over Delhi NCR for this study. We note that in reality each species may show difference in scale height; but such information throughout the year is not available anywhere in the world. CALIOP –derived scale height and aerosol layer thickness are the best possible representations of the aerosol vertical distribution for computing aerosol optical properties.

2.2.2. Internal mixing

In internal mixing, each aerosol particle is composed of all the species and form a homogeneous mixture (Fig. 1, Case 2). We first calculate mass size distribution for all the aerosol components using lognormal distribution:

$$\frac{dM}{dD_p} = \frac{M_t}{(2\pi)^{\frac{1}{2}} D_p \ln \sigma_g} \exp\left(-\frac{(\ln D_p - \ln D_{g,m})^2}{2\ln^2 \sigma_g}\right) \quad (1)$$

where M_t, $D_{g,m}$ and σ_g are total mass, modal diameter and standard deviation of each component. D_p is the diameter of size bin and $D_{g,m}$ is calculated from number mode diameter $D_{g,n}$ using equation from Seinfeld and Pandis (1998):

$$\log(D_{g,m}) = \log(D_{g,n}) + 3(\log \sigma_g)^2 \ln(10) \quad (2)$$

$D_{g,m}$, σ_g and density ρ_g values for the individual aerosol species are obtained from the number size distribution parameters provided in OPAC database (Hess et al., 1998). Dielectric constant, ε_{MG} of the aerosol mixture for each size bin has been calculated using the Maxwell-Garnett mixing rule:

$$\varepsilon_{MG} = \varepsilon_m \left[1 + \frac{3 \sum_{i=1}^{5} f_i \frac{\varepsilon_i - \varepsilon_m}{\varepsilon_i + 2\varepsilon_m}}{1 - \sum_{i=1}^{5} f_i \frac{\varepsilon_i - \varepsilon_m}{\varepsilon_i + 2\varepsilon_m}} \right] \quad (3)$$

Here f_i (i = 5 for five aerosol species) are the respective volume fractions, ε_i are the corresponding dielectric constants (square of refractive indices, $n(\lambda) \pm ik(\lambda)$) and ε_m is the dielectric constant of water. Refractive indices ($n(\lambda)$ and $k(\lambda)$ are real and imaginary parts respectively) of aerosol species are taken from the literature (Shamjad

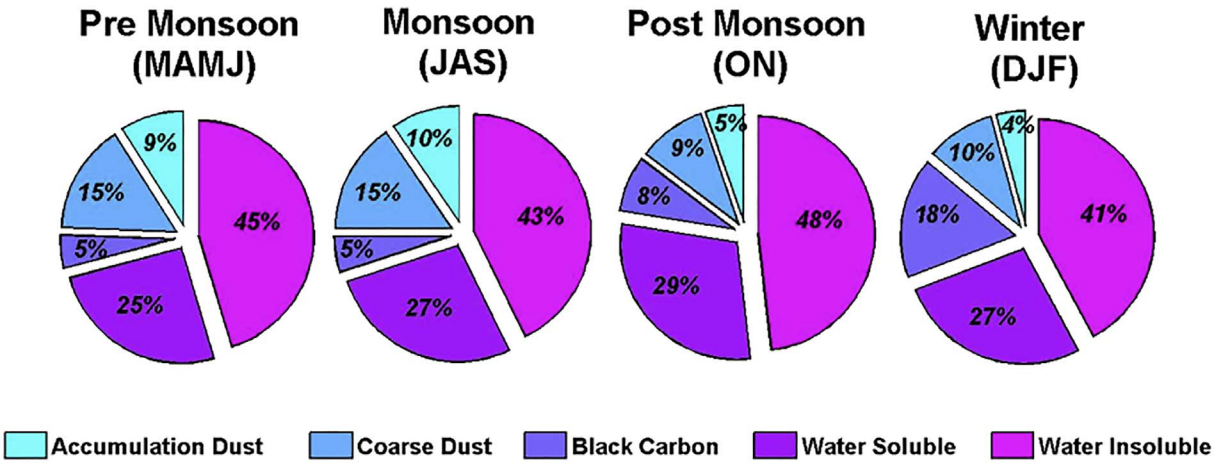

Fig. 2. Seasonal Pie charts representing relative contributions (values shown in %) of five aerosol species to total mass concentration at Delhi NCR.

et al., 2012 and Dey et al., 2006). $n(\lambda)$ at 0.55 μm wavelength are 1.85, 1.40, 1.53 and 1.545 for BC, WS, WINS and dust respectively; while the corresponding values for $k(\lambda)$ are 0.75, 0.6×10^{-7}, 0.0131 and 0.0055. The composite refractive index and size distribution parameters are used in Bohren-Huffman Mie code (Bohren and Huffman, 1983) to calculate spectral optical properties (extinction efficiency - Q_{ext}, scattering efficiency - Q_{sca}, SSA and g). Q_{ext} is converted to extinction coefficient, b_{ext} using:

$$b_{ext} = \pi R_p^2 N Q_{ext} \tag{4}$$

where N is the number concentration of the internally mixed aerosols at the corresponding size (radius, R_p) bin and is calculated by:

$$N = \frac{M}{\frac{4}{3}\pi R_p^3 \rho_g} \tag{5}$$

In Eq. (5), ρ_g is the average density of the mixture, and M is the mass of bulk aerosols obtained from Eq. (1) for the size bin. Composite b_{ext}, and b_{sca} for all the size bins (across the range of R_p, denoted by r in Eqs. (6) and (7)) are calculated as:

$$b_{ext/sca} = \sum_r b_{ext/sca,r} \tag{6}$$

while SSA and g are calculated by:

$$SSA = \frac{\sum_r b_{ext,r} SSA_r}{\sum_r b_{ext,r}} \tag{7}$$

and

$$g = \frac{\sum_r b_{sca,r} g_r}{\sum_r b_{sca,r}} \tag{8}$$

2.2.3. Core-shell mixing

Besides these two mixing states, the third type - 'core-shell mixing' has also been considered, where one component (core) is coated over by another component (shell). Though there is no direct evidence (like SEM image of aerosols) of core-shell mixing in Delhi, previously many studies (e.g. Dey et al., 2008; Srivastava and Ramachandran, 2013; Ramachandran and Srivastava, 2013) showed the possibility of core-shell mixing in the IGB. We considered all possible core-shell combinations of dust, WS, WINS and BC. Firstly, the shell mass is distributed over the core following core size distribution. Shell mass M_s for each size bin is calculated using Eqs. (1) and (2). Number concentration of core species at each size bin is calculated using the same method (eq. 5). Shell radius (R_s) is calculated following Dey et al. (2008):

$$R_s = \left(R_c^3 \frac{\rho_c}{\rho_s} + \frac{3M_s}{4\pi\rho_s N} \right)^{\frac{1}{3}} \tag{9}$$

where, R_c is the core radius for the particular size bin and ρ_s and ρ_c are shell and core density respectively.

R_s, R_c, and refractive indices of core and shell (Shamjad et al., 2012; Dey et al., 2008) are used in Wiscombe code that was developed based on the work by Toon and Ackerman (1981). This code computes the composite aerosol optical properties - Q_{ext}, Q_{sca}, SSA and g for the core-shell mixing. The original code works with the fixed shell radius for a varying core radius. We modified the code to work for the varying core as well as shell radius. Q_{ext} and Q_{sca} are converted to extinction and scattering coefficients respectively using Eq. (4). These core-shell combinations are then externally mixed with remaining aerosol species. For example in Case 3, 'WS coating over dust' is externally mixed with BC and WINS aerosols (Fig. 1). For several core-shell combinations, either the shell-core ratio or the extinction coefficient becomes unrealistically large suggesting that the combination does not seem to be valid for the given mass distributions. Hence we finally choose four realistic core-shell combinations (Fig. 1) - BC coating over dust (case 3), WS coating over dust (case 4), WS coating over WINS (case 5), and BC coating over WINS (case 6) in this study. Hereafter the combinations shown in Case 3 to Case 6 are referred to as 'BC − Dust + WS + WINS', 'WS − Dust + WINS + BC', 'WS − WINS + BC + Dust' and 'BC − WINS + WS + Dust' respectively. We considered all possible core-shell combinations amongst these components, but eliminated some of them except the chosen four (Case 3 to 6) based on abnormally large shell-core ratios, implying unrealistic core-shell mixing for those combinations based on the measured masses of the species.

2.3. Aerosol DRF and heating rate

Aerosol TOA and surface DRF are estimated for all the 6 mixing state cases using the plane parallel radiative transfer model Santa Barbara Discrete Ordinate Radiative Transfer (SBDART) developed by Ricchiazzi et al. (1998). Simulated spectral b_{ext}, SSA and g are used as the inputs in SBDART model to estimate the incoming and outgoing fluxes at the TOA (F_{TOA}) and surface (F_{Sfc}). Other inputs required for the computation - surface albedo and columnar ozone are taken from Ozone Monitoring Instrument (OMI) data, while columnar water vapour is obtained from Moderate Resolution Imaging Spectroradiometer (MODIS). The incoming and outgoing fluxes are estimated for various solar zenith angles in presence and absence of aerosols using SBDART model. The fluxes are then diurnally averaged following previous works (e.g. Dey and Tripathi, 2008):

$$F_{TOA/Sfc} = \frac{1}{2}\int_0^1 F(\mu_0)d\mu_0 \quad (10)$$

where μ_0 is the cosine of solar zenith angle. DRF (ΔF) is calculated using following relation:

$$\Delta F_{TOA/Sfc} = (\Delta F)_{aerosols} - (\Delta F)_{no-aerosols} \quad (11)$$

The atmospheric forcing (ΔF_{atm}) is the difference between TOA and surface DRF, which translates to a net heating rate ($\delta T / \delta t$) in the atmosphere that can be calculated following *Liou* (2002):

$$\frac{\delta T}{\delta t} = \frac{g}{C_p}\frac{\Delta F_{atm}}{\Delta p} \quad (12)$$

where C_p is the specific heat capacity of air at constant pressure, g is the acceleration due to gravity and Δp is the atmosphere pressure difference between the surface and top of the aerosol layer. Δp is calculated based on CALIOP-retrieved aerosol layer thickness for the corresponding month. Vertical profile of heating rate is estimated, by distributing obtained columnar heating rate for the particular month according to the CALIOP-retrieved vertical profile of extinction coefficient (relative to column integrated extinction, b_{ext}).

We analyze the direct measurement of surface irradiance (I_{IMD}) measured at India Meteorological Department for this period in 'clear-sky' condition. This dataset is compared with the surface irradiance calculated for each of these six mixing state cases to infer the most probable mixing state at Delhi NCR.

3. Results and discussion

Mean ($\pm$ 1σ) seasonal surface fluxes measured by IMD in 'clear-sky' condition in Delhi NCR are 273.6 $\pm$ 23.9, 265.9 $\pm$ 23.8, 183.2 $\pm$ 29.5 and 161.2 $\pm$ 26.9 W m^{-2} respectively for the pre-monsoon, monsoon, post-monsoon and winter seasons. We note that although June is considered as a monsoon month in all-India context, monsoon arrives at Delhi NCR by end of June to early July, and hence it is included in the pre-monsoon season in this work. Percentage departure of estimated mean seasonal surface fluxes for various mixing states relative to I_{IMD} is shown in Fig. 3.

During the pre-monsoon season, 'external mixing' case shows the closest match with I_{IMD} (only ~0.82% deviation). The 'WS − WINS + BC + Dust' and 'BC − WINS + WS + Dust' mixing states show slightly higher (~5%) deviation relative to 'external mixing' in this season. Since 'external mixing' is preferably used in satellite retrievals and climate models, we conclude that this choice seems reasonable at Delhi NCR during this season. In the monsoon and winter seasons, 'WS − Dust + BC + WINS' mixing case is the most probable mixing case as it shows the least deviation as compared to I_{IMD} (5.4% and 10.9% respectively). However, 'WS − WINS + WS + Dust' shows least deviation (7.4%) relative to I_{IMD} during the post-monsoon season and hence is inferred as the most probable mixing state for this season. No other mixing case is close enough statistically. We note that 'external mixing', the most preferred case in models is not even close enough in the other three seasons. The positive departure in case of external mixing suggests that if this mixing state is considered, surface irradiance would be biased high. Same is the case for WS − WINS + BC + Dust and BC − WINS + WS + Dust in the monsoon, post-monsoon and winter seasons. Two mixing state cases – internal and BC-Dust + WS + WINS shows large negative departure suggesting that these two cases are highly unlikely in this region.

Though the most probable mixing state is inferred based on the closest match, the minimum deviations vary across the seasons. This may be attributed to several factors. The optical property database may not be exactly accurate. For example, recently Shamjad et al. (2016) have shown that mixing state can change the light absorption capacity of carbonaceous particles. Individual species may have scale heights not exactly similar to each other. Thirdly, the mixing state itself may vary with altitude. Nonetheless, this analysis shows that choice of other mixing states would result in surface irradiance way apart from what is observed and would cause large error in radiative feedback processes in the climate models.

AOD obtained through OPAC assuming external mixing has been compared with AOD retrieved by MISR to assess the fidelity of the aerosol model to infer mixing state. It is observed that OPAC simulated AOD is comparable to MISR-retrieved AOD (Fig. 4) within the retrieval uncertainty except for Jul and Aug. In February and November (though they agree within uncertainty range), mean OPAC AOD is 27.2% and 28.4% higher as compared to the MISR AOD. This is attributed to the fact that BC has large mass fraction in February (26.3%) and November (12.3%). Hence AOD is enhanced due to large absorption, which is not considered in MISR aerosol algorithm (Dey and Di Girolamo, 2010). In July and August, MISR AOD is higher relative to OPAC-simulated AOD due to possible cloud contamination. Also the fact that MISR retrieves AOD only in clear-sky conditions, while chemical data are obtained in both clear and cloudy sky may explain the difference; because AOD is expected to reduce in presence of clouds due to below-cloud (Chowdhury et al., 2016) and wet scavenging. Overall close match (within the expected uncertainty) between the OPAC simulated and MISR retrieved AOD attests the validity of the aerosol model used to infer the most probable aerosol mixing state in Delhi.

Mean seasonal clear-sky DRF at TOA and surface along with the heating rate profiles for all the mixing state cases are shown in Fig. 5 and the values are listed in Table 2 and Table 3. Aerosol TOA and surface DRF change due to changes in extinction coefficient and SSA as mixing state changes. Relative changes in SSA at 0.5 μm with respect to 'external mixing' case are shown in Fig. 6. For all the mixing state cases, 'clear-sky' aerosol DRF is found to be positive at the TOA except for the

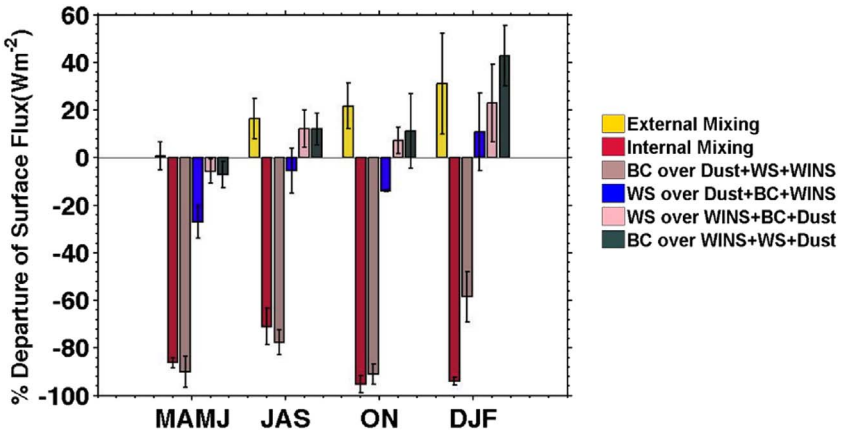

Fig. 3. Percentage departure of mean seasonal surface fluxes of the six mixing state cases with respect to I_{IMD}.

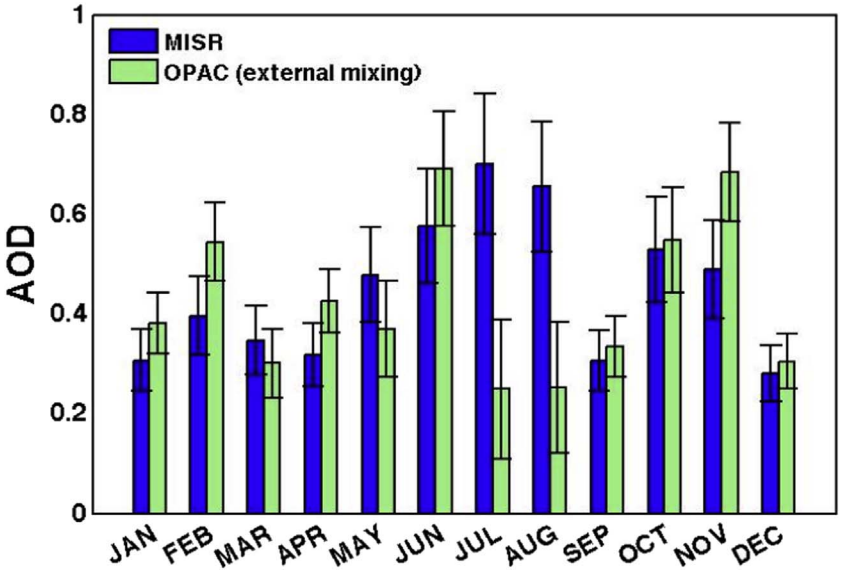

Fig. 4. Comparison of mean monthly AOD from OPAC and MISR over Delhi NCR with the error bars representing the uncertainty range.

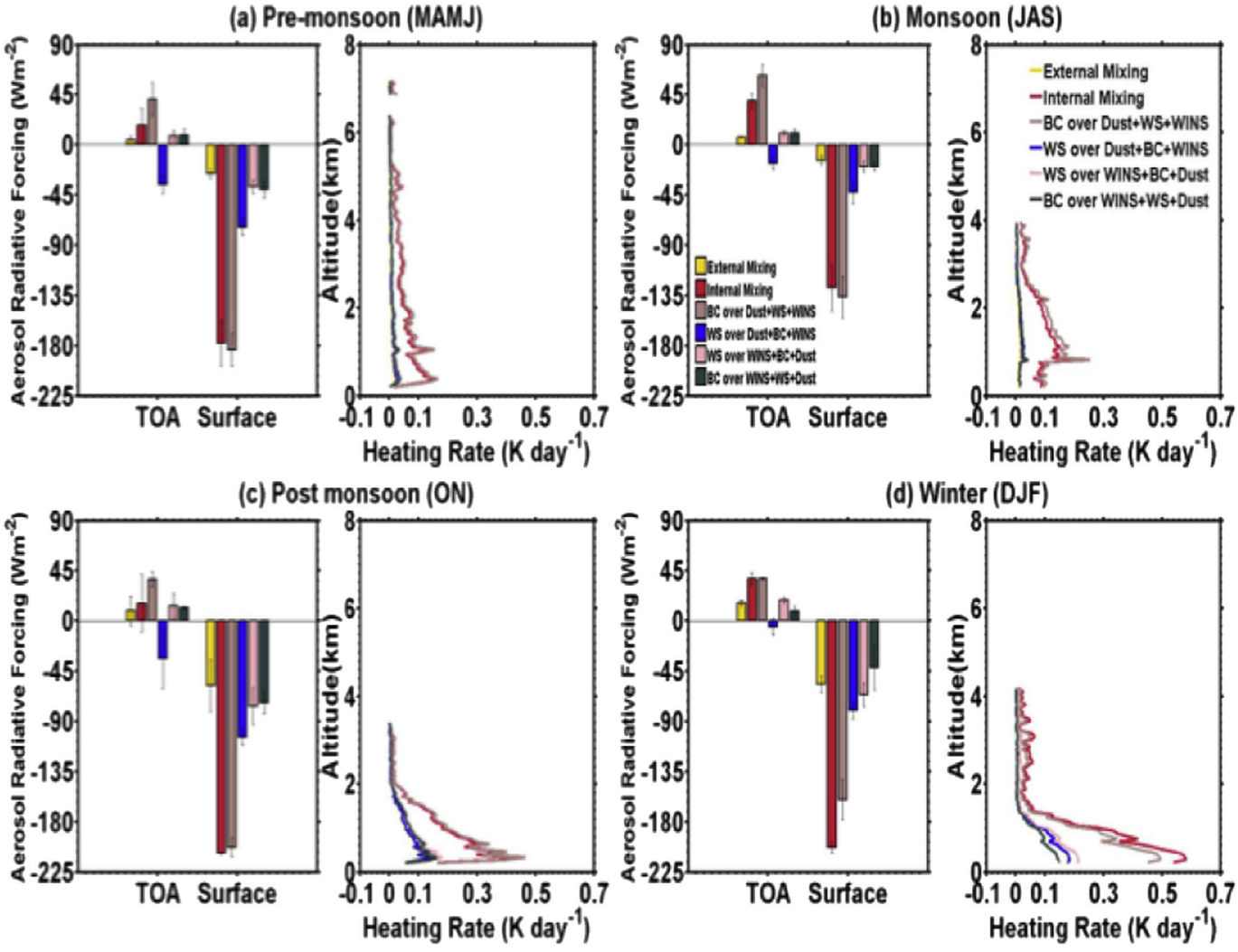

Fig. 5. Seasonal variation of surface and TOA aerosol DRF in clear sky for the six mixing state cases in the (a) pre-monsoon, (b) monsoon, (c) post-monsoon and (d) winter seasons along with the vertical profiles of heating rates (K/day).

Table 2
Mean (± 1σ) seasonal 'clear-sky' aerosol DRF at the TOA (first row) and surface (second row) estimated from the measured aerosol chemical composition at Delhi NCR in north-western India for various aerosol mixing states.

	Winter (Dec–Feb)	Pre-monsoon (Mar–Jun)	Monsoon (Jul–Sep)	Post-monsoon (Oct–Nov)
External mixing	16.2 ± 2.6	4.4 ± 3.9	6.7 ± 0.5	9.1 ± 13.1
	− 56.9 ± 7.4	− 25.9 ± 3.9	− 13.8 ± 4.4	− 58.1 ± 23.6
Internal mixing	37.6 ± 6.0	17.5 ± 15.2	39.4 ± 6.5	15.8 ± 25.8
	− 202.9 ± 4.9	− 177.9 ± 20.2	− 127.9 ± 20.6	− 208.1 ± 0.9
BC − Dust + WS + WINS	38.1 ± 0.8	41.1 ± 14.9	62.3 ± 9.9	37.0 ± 6.7
	− 160.6 ± 18.0	− 183.9 ± 14.9	− 136.2 ± 18.4	− 203.2 ± 8.6
BC − WINS + WS + Dust	18.6 ± 2.3	8.0 ± 4.8	10.7 ± 1.5	13.7 ± 11.4
	− 65.9 ± 10.6	− 37.3 ± 6.2	− 19.5 ± 5.3	− 76.6 ± 16.6
WS − Dust + BC + WINS	− 5.4 ± 7.7	− 35.8 ± 8.0	− 16.3 ± 5.7	− 34.0 ± 26.2
	− 80 ± 7.2	− 74.0 ± 7.6	− 42.4 ± 10.5	− 104.1 ± 7.3
WS − WINS + BC + Dust	9.0 ± 4.2	9.1 ± 5.0	10.7 ± 2.9	11.9 ± 2.1
	− 41.6 ± 19.8	− 40.0 ± 7.2	− 19.5 ± 4.1	− 73.1 ± 10.0

Table 3
Mean (± 1σ) seasonal 'clear-sky' aerosol-induced heating rates (in K/day) estimated from the measured aerosol chemical composition at Delhi NCR in north-western India for various aerosol mixing states.

	Winter (Dec–Feb)	Pre-monsoon (Mar–Jun)	Monsoon (Jul–Sep)	Post-monsoon (Oct–Nov)
External mixing	3.0 ± 2.1	0.5 ± 0.1	0.5 ± 0.1	1.7 ± 1.0
Internal mixing	9.6 ± 5.6	3.3 ± 0.8	4.1 ± 0.7	5.7 ± 0.9
BC − Dust + WS + WINS	7.9 ± 5.6	3.8 ± 0.6	4.8 ± 0.7	6.1 ± 0.2
BC − WINS + WS + Dust	3.5 ± 2.5	0.8 ± 0.2	0.7 ± 0.2	2.3 ± 0.8
WS − Dust + BC + WINS	3.1 ± 2.1	0.7 ± 0.1	0.6 ± 0.2	1.8 ± 0.9
WS − WINS + BC + Dust	2.3 ± 2.0	0.8 ± 0.2	0.7 ± 0.2	2.1 ± 0.1

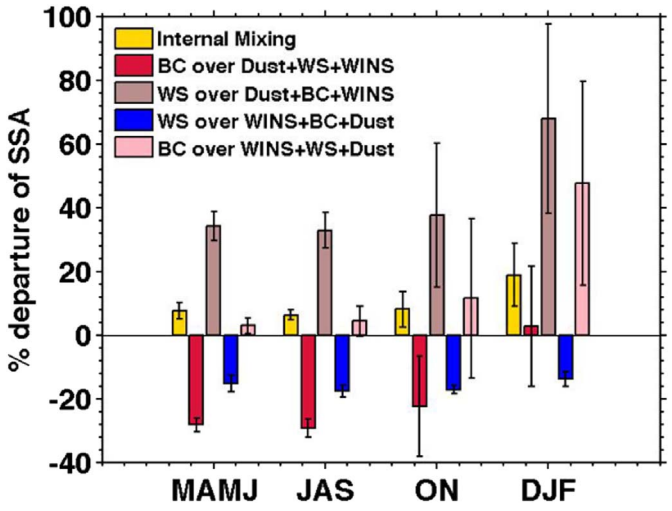

Fig. 6. Relative changes (in %) in aerosol SSA with respect to external mixing. Error bars represent ± 1 standard deviation around mean values.

'WS − Dust + BC + WINS' mixing case, when TOA DRF switches to cooling. This can be attributed to large (> 30%) enhancement in SSA due to enhanced scattering cross-section for dust particles coated by WS. The assumption of external mixing in the seasons other than pre-monsoon would bias the TOA aerosol DRF to warming. DRF is larger (more positive) for 'internal mixing' state than the 'external mixing' because the overall extinction is enhanced manifold overcompensating a slight increase in SSA. As a result, TOA warming increases by 1.7 to 5.9 times.

BC coating over dust enhances the effective cross-section area of absorption at every size bin resulting in the largest enhancement in DRF at the TOA for the case of 'BC − Dust + WS + WINS'. Largest reduction in SSA for this mixing state case (Fig. 6) confirms this explanation. TOA warming is enhanced for BC coating over WINS, but not by same magnitude as of BC coating over dust because of much thinner BC shell over WINS relative to dust (as core); since the mass of WINS is much larger than that of dust and hence distributing same BC mass to coat much larger WINS particles compared to dust would require much thinner shell. Similarly shell thickness of WS coating over WINS is also small. Since this WS-WINS combination is externally mixed with BC and dust (two absorbing components), the SSA reduces with respect to external mixing; while external mixing of dust and WS with BC − WINS enhances scattering relative to external mixing, as evidenced in the increase in SSA. However, b_{ext} is larger for BC − WINS + WS + Dust compared to WS-WINS + BC + Dust; therefore leading to similar TOA DRF. In case of internal mixing, extinction coefficient increases manifold causing largest surface dimming.

For the most probable mixing states, mean seasonal TOA aerosol DRF are 4.4 ± 3.9 (external mixing), − 16.3 ± 5.7 and − 5.4 ± 7.7 (WS − Dust + BC + WINS) and 13.6 ± 11.4 (WS − WINS + BC + Dust) W m^{-2} respectively for the pre-monsoon, monsoon, winter and post-monsoon seasons. The corresponding mean surface aerosol DRF are − 25.9 ± 3.9 (external mixing), − 42.4 ± 10.5 and − 80.0 ± 7.2 (WS − Dust + BC + WINS) and − 76.6 ± 16.6 (WS − WINS + BC + Dust) W m^{-2} respectively. Similar to aerosol DRF at TOA, surface DRF shows large variation with change in mixing state. For example, surface DRF increases for all other mixing states compared to that for external mixing, simply because attenuation of solar radiation by each individual particle increases if particles are internally mixed or one composition coats over another. The least surface dimming is observed for 'external' mixing followed by 'BC − WINS + WS + Dust' case. The surface dimming for 'internal mixing' and 'BC − Dust + WS + WINS' are very high and comparable in all the seasons. While each internally mixed particle absorbs and scatters solar radiation, larger effective absorption cross-section for BC – Dust + WS + WINS lead to such larger surface DRF. Relatively higher enhancement in surface DRF is observed during the pre-monsoon (6.9 times) and monsoon (9.3 times) compared to the post-monsoon and winter seasons (3.6 times) for the internal mixing case. The heating rate profiles follow similar pattern across the seasons. Large (> 0.3 K/day) heating is observed within the boundary layer for 'internal mixing' and 'BC − Dust + WS + WINS' case, more than double than the rest of the mixing cases. Note that aerosols are mostly confined within 4 km in the post-monsoon to winter seasons at Delhi NCR, while the aerosol layer expands in the pre-monsoon season. In the monsoon season, aerosol retrieval above 4 km has large uncertainty due to presence of monsoon clouds.

Previously, Dey et al. (2008) have examined the probable mixing state in Kanpur, which is an urban site situated in the Central IGB

situated at ~500 km southeast of Delhi. Comparative analysis of the results from Delhi and Kanpur suggests that core-shell mixing is prevalent over a large stretch of the IGB in the post-monsoon season. The analysis was not carried out for the monsoon season in Kanpur, and hence the spatial extent of core-shell mixing cannot be determined. While 'core-shell' mixing seems to be the mixing state in the western IGB, WS coating over WINS particles does not occur in the Central IGB, perhaps because of much lesser WINS component in bulk aerosols (Dey and Tripathi, 2007). We hypothesize that since Delhi is closer (than Kanpur) to the dust source regions, less time is available to coat dust particles as they are transported to Delhi. Hence external mixing seems to be the probable mixing state in Delhi in the pre-monsoon season. Sufficient time is available to coat dust particles by BC as they are transported to further (500 km west of Delhi) downwind to Kanpur. Hence BC − Dust + WS + WINS was the preferred case in Kanpur (Dey et al., 2008). Aerosol characteristics in the eastern IGB is limited (Pani and Verma, 2014) and similar analysis is required to fully understand the spatial extent of aerosol processing via mixing in this polluted region.

Key assumptions and uncertainties involved in the work warrant detailed discussion. We note that the most probable mixing state is inferred by matching the simulated surface downward flux with measured one. This approach is adopted because of lack of measured aerosol optical properties (e.g. AOD, SSA and *g*) during the study period. The surface reaching flux is computed by radiative transfer model using the simulated optical properties that utilize OPAC database. Earlier, we observed that OPAC aerosol size distribution parameters are within ± 15% of measured parameters at least in the winter season in the central IGB (Dey and Tripathi, 2007). No such database is available from western IGB even for a single season. This translates into 20% uncertainty in computed flux. The differences in the aerosol DRF (and of flux) for other mixing states from the external mixing are larger in view of the measured flux considering the uncertainty. Therefore, we believe that our interpretations hold true in general.

Our results have important climatic implications in the context of existing studies on aerosol-climate interaction in the Indian subcontinent. We show that aerosol TOA and surface DRF vary drastically due to change in mixing state. Large modulation in aerosol DRF, presented here, implies that any change in mixing state would contribute to large error in estimated DRF. Most of the models, if not all, assume external mixing (e.g. Kedia et al., 2016) that may lead to a bias in aerosol DRF and feedback processes. Similar efforts are required at other parts of the country to assess the validity of the assumption of external mixing in determining aerosol DRF. This can only be achieved if we have robust chemical composition of aerosols. Mostly in India, aerosol composition is inferred from optical measurements (Satheesh and Srinivasan, 2006) and hence it is difficult to disentangle the modulation of aerosol DRF by mixing state (via atmospheric processing) from the modulation of DRF due to uncertainty in inferred composition. This issue needs to be addressed in details.

4. Summary and conclusions

We examine and report the modulation of aerosol DRF at Delhi NCR (an urban site in the Indo-Gangetic Basin in northern India) by mixing state in clear-sky condition utilizing measured aerosol composition for two years period (2007–2008).

The main findings are summarized as follows:

1. External mixing, the preferred choice in models and in estimation of aerosol DRF, seems valid only in the pre-monsoon season in Delhi NCR.
2. 'WS coating over dust' externally mixed with BC and WINS is inferred as the most probable mixing state in the winter and monsoon seasons; while 'WS coating over WINS' externally mixed with BC and dust appears to be the preferred mixing state during the post-monsoon season.
3. Aerosol dimming increases if external mixing changes to either internal mixing or any combination of core-shell mixing, because of enhancement in extinction cross-section. Largest increase is observed for internal mixing and 'BC coating over dust' externally mixed with WS and WINS because of largest decrease in SSA.
4. Aerosol TOA warming tends to increase in all mixing state cases (relative to external mixing) except 'WS coating over dust' externally mixed with BC and WINS, where TOA DRF switches to cooling because of enhanced scattering.
5. Mean seasonal TOA aerosol DRF for the inferred most probable mixing states are 4.4 ± 3.9, −16.3 ± 5.7, 13.6 ± 11.4 and −5.4 ± 7.7 W m^{-2} respectively for the pre-monsoon, monsoon, post-monsoon and winter seasons; while the corresponding surface DRFs are −25.9 ± 3.9, −42.4 ± 10.5, −76.6 ± 16.6, and −80.0 ± 7.2 W m^{-2} in Delhi NCR.

Acknowledgements

The work is partially supported by grant from Climate Change Program of Department of Science and Technology, Govt. of India under contract DST/CCP/PR/11/2011 through research project operational at IIT Delhi (RP2580). We thank the anonymous reviewers for constructive comments that helped improving the manuscript.

References

Bohren, C, Huffman, D. 1983. Absorption and scattering of light by small particles. doi:https://doi.org/10.1002/9783527618156.

Boucher, O., Randall, D., Artaxo, P., Bretherton, C., Feingold, G., Forster, P., Kerminen, V.-M., Kondo, Y., Liao, H., Lohmann, U., Rasch, P., Satheesh, S.K., Sherwood, S., Stevens, B., Zhang, X.Y., 2013. Clouds and Aerosols, Working Group I Contribution to the Fifth Assessment Report of the Intergovernmental Panel on Climate Change. pp. 571–658. http://dx.doi.org/10.1017/cbo9781107415324.016.

Chandra, S., Satheesh, S.K., Srinivasan, J., 2004. Can the state of mixing of black carbon aerosols explain the mystery of 'excess' atmospheric absorption? Geophys. Res. Lett. 31, L19109. http://dx.doi.org/10.1029/2004GL020662.

Collaud Coen, M., et al., 2010. Minimizing light absorption measurement artifacts of the Aethalometer: evaluation of five correction algorithms. Atmos. Meas. Tech. 3, 457–474. http://dx.doi.org/10.5194/amt-3-457-2010.

Chowdhury, S., Dey, S., Ghosh, S., Saud, T., 2016. Satellite-based estimates of aerosol washout and recovery over India during monsoon. Aerosol Air Qual. Res. 16, 1302–1314.

Dey, S., Di Girolamo, L., 2010. A climatology of aerosol optical and microphysical properties over the Indian subcontinent from 9 years (2000–2008) of Multiangle Imaging Spectroradiometer (MISR) data. J. Geophys. Res. Atmos. 115, 1–22. http://dx.doi.org/10.1029/2009JD013395.

Dey, S., Tripathi, S.N., 2007. Estimation of aerosol optical properties and radiative effects in the Ganga basin, northern India, during the wintertime. J. Geophys. Res. Atmos. 112, 1–16. http://dx.doi.org/10.1029/2006JD007267.

Dey, S., Tripathi, S.N., 2008. Aerosol direct radiative effects over Kanpur in the Indo-Gangetic basin, northern India: long-term (2001–2005) observations and implications to regional climate. J. Geophys. Res. Atmos. 113, 1–20. http://dx.doi.org/10.1029/2007JD009029.

Dey, S., Tripathi, S.N., Singh, R.P., Holben, B.N., 2006. Retrieval of black carbon and specific absorption over Kanpur city, northern India during 2001–2003 using AERONET data. Atmos. Environ. 40, 445–456. http://dx.doi.org/10.1016/j.atmosenv.2005.09.053.

Dey, S., Tripathi, S.N., Mishra, S.K., 2008. Probable mixing state of aerosols in the Indo-Gangetic Basin, northern India. Geophys. Res. Lett. 35, 1–5. http://dx.doi.org/10.1029/2007GL032622.

Dey, S., Di Girolamo, L., Zhao, G., Jones, A., McFarquhar, G., 2011. Satellite-observed relationships between aerosol and trade-wind cumulus cloud properties over the Indian Ocean. Geophys. Res. Lett. 38. http://dx.doi.org/10.1029/2010gl045588.

Dumka, U., Tripathi, S.N., Misra, A., Giles, D., Eck, T., Sagar, R., Holben, B., 2014. Latitudinal variation of aerosol properties from Indo-Gangetic Plain to central Himalayan foothills during TIGERZ campaign. J. Geophys. Res.-Atmos. 119, 4750–4769. http://dx.doi.org/10.1002/2013jd021040.

Hansen, A., Rosen, H., Novakov, T., 1984. The Aethalometer—an instrument for the real-time measurement of optical absorption by Aerosol particles. Sci. Total Environ 36, 191–196.

Hess, M., Koepke, P., Schult, I., 1998. Optical properties of aerosols and clouds: the software package OPAC. Bull. Am. Meteorol. Soc. 79, 831–844. http://dx.doi.org/10.1175/1520-0477(1998)079<0831:OPOAAC>2.0.CO;2.

Jacobson, M., 2001. Strong radiative heating due to the mixing state of black carbon in atmospheric aerosols. Nature 409, 695–697. http://dx.doi.org/10.1038/35055518.

Jacobson, M., Hansson, H., Noone, K., Charlson, R., 2000. Organic atmospheric aerosols:

review and state of the science. Rev. Geophys. 38, 267–294. http://dx.doi.org/10.1029/1998rg000045.
Kahn, R., Gaitley, B., Garay, M., Diner, D., Eck, T., Smirnov, A., Holben, B., 2010. Multiangle Imaging SpectroRadiometer global aerosol product assessment by comparison with the Aerosol Robotic Network. J. Geophys. Res. 115. http://dx.doi.org/10.1029/2010jd014601.
Kedia, S., Cherian, R., Islam, S., Das, S.K., Kaginalkar, A., 2016. Regional simulation of aerosol radiative effects and their influence on rainfall over India using WRF-Chem model. Atmos. Res. 182, 232–242.
Krishna Moorthy, K., Suresh Babu, S., Manoj, M.R., Satheesh, S.K., 2013. Buildup of aerosols over the Indian Region. Geophys. Res. Lett. 40, 1011–1014. http://dx.doi.org/10.1002/grl.50165.
Liou, K., 2002. An Introduction to Atmospheric Radiation. Academic Press, Amsterdam.
Lodhi, N., Beegum, S., Singh, S., Kumar, K., 2013. Aerosol climatology at Delhi in the western Indo-Gangetic Plain: microphysics, long-term trends, and source strengths. J. Geophys. Res.-Atmos. 118, 1361–1375. http://dx.doi.org/10.1002/jgrd.50165.
Mishchenko, M., Geogdzhayev, I., Rossow, W., Cairns, B., Carlson, B., Lacis, A., Liu, L., Travis, L., 2007. Long-term satellite record reveals likely recent aerosol trend. Science 315, 1543. http://dx.doi.org/10.1126/science.1136709.
More, S., Pradeep Kumar, P., Gupta, P., Devara, P.C.S., Aher, G.R., 2013. Comparison of aerosol products retrieved from AERONET, MICROTOPS and MODIS over a Tropical Urban City, Pune, India. Aerosol Air Qual. Res. http://dx.doi.org/10.4209/aaqr.2012.04.0102.
Pani, S.K., Verma, S., 2014. Variability of wintertime and summertime aerosols over eastern India urban environment. Atmos. Res. 137, 112–124.
Perrino, C., Tiwari, S., Catrambone, M., Dalla Torre, S., Rantica, E., Canepari, S., 2011. Chemical characterization of atmospheric PM in Delhi, India, during different periods of the year including Diwali festival. Atmos. Pollut. Res. 2, 137–147. http://dx.doi.org/10.5094/apr.2011.048.
Ram, K., Sarin, M., 2010. Spatio-temporal variability in atmospheric abundances of EC, OC and WSOC over Northern India. J. Aerosol Sci. 41, 88–98. http://dx.doi.org/10.1016/j.jaerosci.2009.11.004.
Ramachandran, S., Kedia, S., 2010. Black carbon aerosols over an urban region: radiative forcing and climate impact. J. Geophys. Res. 115. http://dx.doi.org/10.1029/2009jd013560.
Ramachandran, S., Srivastava, R., 2013. Influences of external vs. core-shell mixing on aerosol optical properties at various relative humidities. Environ. Sci.: Processes Impacts 15, 1070–1077.
Ricchiazzi, P., Yang, S., Gautier, C., Sowle, D., 1998. SBDART: a research and teaching software tool for plane-parallel radiative transfer in the earth's atmosphere. Bull. Am. Meteorol. Soc. 79, 2101–2114. http://dx.doi.org/10.1175/1520-0477(1998)079<2101:sarats>2.0.co;2.
Safai, P.D., Devara, P.C.S., Raju, M.P., Vijayakumar, K., Rao, P.S.P., 2014. Relationship between black carbon and associated optical, physical and radiative properties of aerosols over two contrasting environments. Atmos. Res. 149, 292–299. http://dx.doi.org/10.1016/j.atmosres.2014.07.006.
Samiksha, S., Raman, R.S., Nirmalkar, J., Kumar, S., Sirvaiya, R., 2017. PM_{10} and $PM_{2.5}$ chemical source profiles with optical attenuation and health risk indicators of paved and unpaved road dust in Bhopal, India. Environ. Pollut. 222, 477–485.
Sanap, S.D., Pandithurai, G., 2015. The effect of absorbing aerosols on Indian summer monsoon circulation and rainfall: a review. Atmos. Res. 164-165, 318–327.
Satheesh, S.K., Srinivasan, J., 2006. A method to estimate Aerosol radiative forcing from spectral optical depths. J. Atmos. Sci. 63, 1082–1092.
Seinfeld, J., Pandis, S., 1998. Atmospheric Chemistry and Physics. Wiley, New York.
Shamjad, P.M., Tripathi, S.N., Aggarwal, S.G., Mishra, S.K., Joshi, M., Khan, A., Sapra, B.K., Ram, K., 2012. Comparison of experimental and modelled absorption enhancement by Black Carbon (BC) cored polydisperse aerosols under hygroscopic conditions. Environ. Sci. Technol. 46, 8082–8089. http://dx.doi.org/10.1021/es300295v.
Shamjad, P.M., Tripathi, S.N., Thamban, N.M., Vreeland, H., 2016. Refractive index and absorption attribution of highly absorbing brown carbon aerosols from an urban Indian city Kanpur. Sci Rep 6, 37735.
Singh, S., Nath, S., Kohli, R., Singh, R., 2005. Aerosols over Delhi during pre-monsoon months: characteristics and effects on surface radiation forcing. Geophys. Res. Lett. 32, L13808. http://dx.doi.org/10.1029/2005GL023062.
Singh, S., Soni, K., Bano, T., Tanwar, R.S., Nath, S., Arya, B.C., 2010. Clear-sky direct aerosol radiative forcing variations over mega-city Delhi. Ann. Geophys. 28, 1157–1166. http://dx.doi.org/10.5194/angeo-28-1157-2010.
Srivastava, R., Ramachandran, S., 2013. The mixing state of aerosols over the Indo-Gangetic Plain and its impact on radiative forcing. Q. J. R. Meteorol. Soc. 139, 137–151. http://dx.doi.org/10.1002/qj.1958.
Srivastava, A.K., Singh, S., Tiwari, S., Bisht, D.S., 2012. Contribution of anthropogenic aerosols in direct radiative forcing and atmospheric heating rate over Delhi in the Indo-Gangetic Basin. Environ. Sci. Pollut. Res. 19 (4), 1144–1158.
Srivastava, A., Soni, V., Singh, S., Kanawade, V., Singh, N., Tiwari, S., Attri, S., 2014a. An early South Asian dust storm during March 2012 and its impacts on Indian Himalayan foothills: a case study. Sci. Total Environ. 493, 526–534. http://dx.doi.org/10.1016/j.scitotenv.2014.06.024.
Srivastava, P., Dey, S., Agarwal, P., Basil, G., 2014b. Aerosol characteristics over Delhi national capital region: a satellite view. Int. J. Remote Sens. 35, 5036–5052.
Tare, V., et al., 2006. Measurements of atmospheric parameters during Indian Space Research Organization Geosphere Biosphere Program Land Campaign II at a typical location in the Ganga Basin: 2. Chemical properties. J. Geophys. Res. 111. http://dx.doi.org/10.1029/2006jd007279.
Tiwari, S., Pandithurai, G., Attri, S.D., Srivastava, A.K., Soni, V.K., Bisht, D.S., Anil Kumar, V., Srivastava, M.K., 2015. Aerosol optical properties and their relationship with meteorological parameters during wintertime in Delhi, India. Atmos. Res. 153, 465–479.
Toon, O., Ackerman, T., 1981. Algorithms for the calculation of scattering by stratified spheres. Appl. Opt. 20, 3657. http://dx.doi.org/10.1364/ao.20.003657.
Tripathi, S., Srivastava, A., Dey, S., Satheesh, S., Krishnamoorthy, K., 2007. The vertical profile of atmospheric heating rate of black carbon aerosols at Kanpur in northern India. Atmos. Environ. 41, 6909–6915. http://dx.doi.org/10.1016/j.atmosenv.2007.06.032.
Tyagi, S., Tiwari, S., Mishra, A., Singh, S., Hopke, P.K., Singh, S., Attri, S.D., 2017. Characteristics of absorbing aerosols during winter foggy period over the National Capital Region of Delhi: impact of planetary boundary layer dynamics and solar radiation flux. Atmos. Res. 188, 1–10.
Virkkula, A., Mäkelä, T., Yli-Tuomi, T., Hirsikko, A., Kopo- nen, I. K., Hämeri, K., and Hillamo, R., 2007. A simple procedure for correcting loading effects of aethalometer data. J. Air Waste Manage. Assoc. 57, 1214–1222. http://dx.doi.org/10.3155/1047-3289.57.10.1214.
Virkkula, A., Chi, X., Ding, A., Shen, Y., Nie, W., Qi, X., Zheng, L., Huang, X., Xie, Y., Wang, J., Petaja, T., Kulmala, M., 2015. On the interpretation of the loading correction of the aethalometer. Atmos. Meas. Tech. 8, 4415–4427.
Wang, T., Li, S., Shen, Y., Deng, J., Xie, M., 2010. Investigations on direct and indirect effect of nitrate on temperature and precipitation in China using a regional climate chemistry modelling system. J. Geophys. Res. 115. http://dx.doi.org/10.1029/2009jd013264.
Weingartner, E., Saathoff, H., Schnaiter, M., Streit, N., Bitnar, B., Baltensperger, U., 2003. Absorption of light by soot particles: determination of the absorption coefficient by means of aethalometers. J. Aerosol Sci. 34, 1445–1463. http://dx.doi.org/10.1016/s0021-8502(03)00359-8.